Catalysis Today 168 (2011) 118–123

Contents lists available at ScienceDirect

Catalysis Today

journal homepage: www.elsevier.com/locate/cattod

A mechanistic study on the synthesis of MCM-22 from SBA-15 by dry gel conversion to form a micro- and mesoporous composite

Masaru Ogura*, Kazuya Inoue, Taiji Yamaguchi

Institute of Industrial Science, The University of Tokyo, Komaba 4-6-1, Meguro, Tokyo 153-8505, Japan

ARTICLE INFO

Article history:
Received 7 October 2010
Received in revised form
30 November 2010
Accepted 25 December 2010
Available online 11 February 2011

Keywords:
Microporous and mesoporous composite
Zeolite
MCM-22
Micropocket
Vapor-phase transport

ABSTRACT

A composite material with ordered pores in both the micro- and mesopore ranges was prepared by a dry gel conversion technique known as vapor-phase transport (VPT). Mesoporous silica SBA-15 was used as the SiO_2 source, and sodium aluminate was used as the Al_2O_3 source on the silica. VPT was then carried out under an atmosphere of hexamethyleneimine and water vapors. The unique microporous structure of MCM-22, a micropocket on the external surface of the zeolite, was generated at a late stage of crystallization. A zeolitic acid site, as strong as that of MCM-22 with mesopores originated from SBA-15, was achieved to create before the long-range ordering of the zeolite. A building unit of the zeolite was also formed at an early stage of crystallization. A drastic change in the morphology of SBA-15, promoted with the help of water vapor, took place during the course of crystallization. Slow crystallization and a structural support (e.g., carbon) inside the mesopores are necessary to prevent collapse of the mesostructure derived from the original SBA-15, and to obtain an ordered micro- and mesoporous composite material.

1. Introduction

Hierarchically porous silica-based structures, known as composite porous silicate materials or mesoporous zeolites, are attracting considerable attention based on the demand for catalysts that treat bulky molecules in petrochemical processes. A large variety of such composite materials can be found in the literature [1–13]. More recently, such materials have even been reported at relevant international conferences, showing that they are currently being applied to various kinds of catalytic reactions. Such materials, if realized, would be one of the key materials in recent decades to meet the numerous challenges posed by environmental crises and resource management.

From a broad overview of these studies, we can divide such materials into two categories: composite materials, which can be synthesized through a bottom-up approach using nanocrystalline zeolites, and mesoporous zeolite, which is prepared by a post-synthesis, top-down approach by treatment with a highly alkaline solution to partially dissolve the zeolite. However, it is difficult to find a material, in the real sense of a composite, which is suffused with pores in both the micro- and mesopore ranges. Furthermore, in the application of such materials in the literature, kinetic reactions, such as the cracking of bulky molecules, are normally adopted. However, there are few examples that apply such materials in thermodynamic reactions that are governed by an equilibrium established among some products, whose selective production is favored by existence of micropores and mesopores. This is mainly because many of the composite materials obtained so far are composed of a zeolitic strong-acid site and mesospaces.

Our approach to obtain composite materials with micro- and mesopores can be summarized as follows (Scheme 1): use mesoporous silica for the starting material as a source of SiO_2, and perform a partial phase transformation of the amorphous mesopore wall into crystalline silicate by a dry gel conversion technique called vapor-phase transport [14]. We can tune the mesostructure by selecting a type of mesoporous silica, and tune the zeolitic nature by changing the organic structure-directing agent (OSDA) supplied from the vapor phase during the course of crystallization. The possibility of zeolite and the mesoporous material mixing physically can be avoided by this method, because nucleation always occurs on the mesopore wall by using it as a silica source. On the other hand, excess growth of zeolite on the wall results in collapse of the ordered mesostructure; therefore, carbonization inside the mesopores is quite important to support the structure. Additionally, the role of the carbon in controlling the diffusion of OSDA to an acidic nucleation site has been clarified. Nonetheless, the composite material obtained by this method is one of a site and mesospaces rather than one of micro- and mesospaces.

MCM-22 is a zeolite within which exists a large ordered microvoid that faces the outer surface through ten-membered ring channels [15]. The inner microspace serves as a half-cup microp-

* Corresponding author. Tel.: +81 3 54526321; fax: +81 3 54526322.
E-mail address: oguram@iis.u-tokyo.ac.jp (M. Ogura).

0920-5861/$ – see front matter © 2011 Elsevier B.V. All rights reserved.
doi:10.1016/j.cattod.2010.12.046

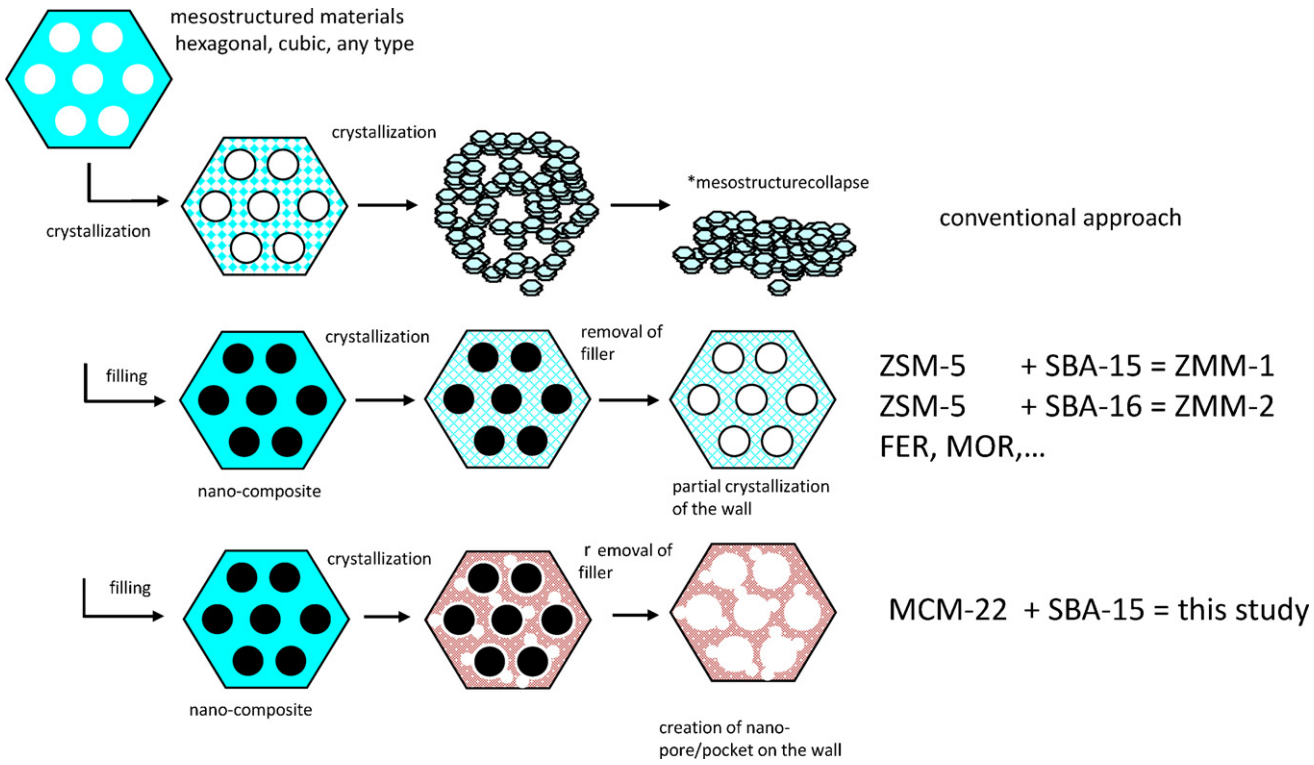

Scheme 1. Schematic image of our approach for composite synthesis by use of VPT method.

ocket when exposed to the external surface of the crystal. The unique and well-known catalytic performance of this zeolite—of selectively forming a mono-alkylated product during alkylation of benzene by ethylene or propylene into ethylbenzene or cumene (isopropyl benzene), respectively—derives from its microstructure [16], which is believed to control residence and selective adsorption on the crystal.

In this study, we focus on the zeolite MCM-22 as a material to provide micropockets. SBA-15 is used as a source of mesopores. With our methodology, MCM-22-like micropockets are constructed on the thick wall of mesopores in SBA-15. Successful preparation will be tested by adsorption of aromatic compounds, which is superior to catalysis in evaluating selective adsorption in the micropockets on the internal mesopores.

2. Experimental

2.1. Synthesis of SBA-15

The block copolymer P123 (BASF) was used as the active surfactant for mesoporous silica SBA-15 with good reproducibility. Four grams of P123 were dissolved into 30 g of water and 120 g of 2 M HCl under vigorous stirring at 40 °C. After the mixture became clear, 8.5 g of tetraethylorthosilicate (TEOS) was poured into the solution with continued stirring. The resultant mixture was agitated at 40 °C for 20 h, and then heated at 100 °C for 24 h. Calcination under an air stream was carried out to regenerate mesopores filled with the surfactant at 500 °C, and at 900 °C for further dehydration of the product.

2.2. Synthesis of MCM-22 by vapor-phase transport

Synthesis of MCM-22 by vapor-phase transport (VPT) was performed according to the previous report by Inagaki et al. [17]. Hexamethyleneimine (HMI) was used as the organic structure-directing agent (OSDA) for MCM-22. The hydrogel composition was as follows: SiO_2: 0 or 0.15 NaOH: 0.028 Al_2O_3: 44H_2O. First, the hydrogel was stirred at room temperature for 30 min for equilibration. The hydrogel was then heated with stirring at ca. 70 °C until the gel was dried into powder. The dried hydrogel (0.2 g) was placed in the middle of a 50 mL Teflon-lined pressure container, separated from the mixture of 2.0 g of water and 1.5 g of HMI to prevent direct contact. The volume of water was varied by supplying less (0.12 g) or an excess amount (2.0 g). The container was then closed tightly and kept in an air oven preheated typically at 150 °C for 7–21 days. Calcination to remove the OSDA in the micropores was conducted under an air stream at 540 °C for 5 h.

The synthesis of MCM-22 from SBA-15 was performed using hydrogels of the same composition but using SBA-15 instead of TEOS as the SiO_2 source.

In case of MCM-22 synthesis by the hydrothermal method, hydrogels of the same composition, but using a fumed SiO_2 powder, were heated in the same pressure container at the same temperature as in VPT synthesis with a rotation speed of 25 rpm.

3. Results and discussion

3.1. VPT synthesis of MCM-22 with SBA-15 as the Si source

First, the typical XRD patterns of products crystallized by VPT of SBA-15 are summarized in Fig. 1. The parent SBA-15 sample used in this study showed the typical pattern, including three distinct diffractions that correspond to a periodic 2*d*-hexagonal structure. The pattern was retained even after loading sodium aluminate on the SBA-15. However, it is difficult to maintain the mesostructure after crystallizing SBA-15 into its zeolitic phase of MCM-22(P) via VPT without a support such as carbon filled inside the mesopores.

Table 1 summarizes a series of MCM-22 preparations obtained by the conventional hydrothermal method and by VPT from SBA-15. Recall that there is no difference in the physicochemical

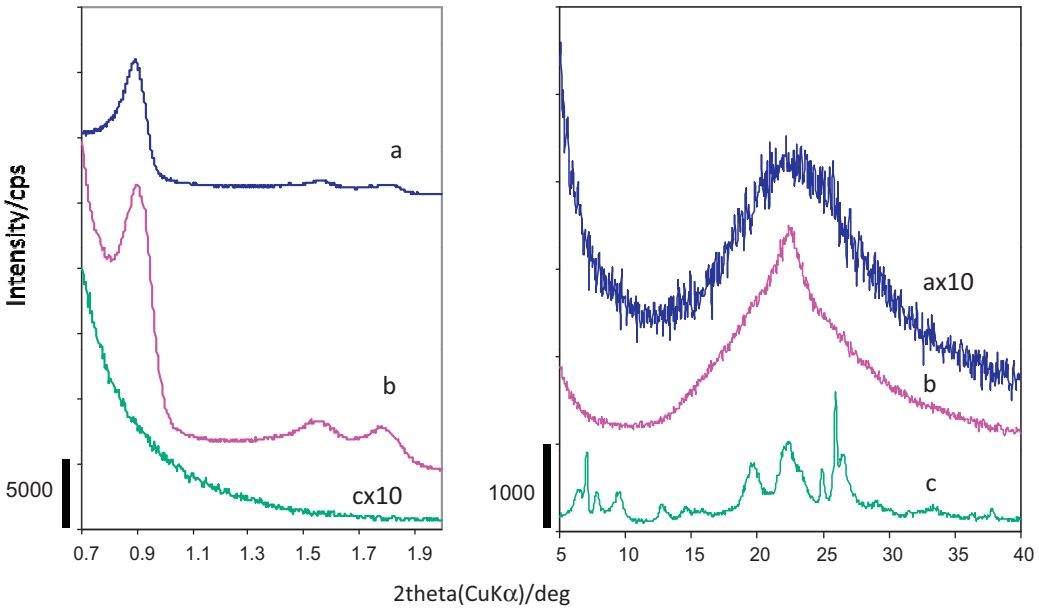

Fig. 1. The XRD pattern of (a) parent SBA-15, (b) Al/SBA-15, and (c) (b)+VPT7 days.

Table 1
Conditions for MCM22/SBA15 composite synthesis.

Entry no.	Silica source	+Al, Na sources	Dried gel structure	150 °C, 7d crystallization	Final phase		Particle morphology
					Meso	Zeolite	
1	Fumed silica	$NaAlO_2$ NaOH	–	HMI/H_2O-hydrothermal	None	MCM-22(P)	Agglomerates of thin film (MCM-22)
2	SBA15	$NaAlO_2$ NaOH	2d hexagonal	HMI/H_2O VPT	None	MCM-22(P)	Agglomerates of thin film
3	SBA15	$NaAlO_2$	2d hexagonal	HMI/H_2O VPT	None	MCM-22(P)	Agglomerates of thin film
4	SBA15 900 °C	$NaAlO_2$	2d hexagonal	HMI/H_2O VPT	None	MCM-22(P)	Agglomerates of thin film
5	SBA15	$NaAlO_2$	2d hexagonal + HMI	H_2O SAC	None	Amorphous	Sausage-like long chain (SBA-15)
6	SBA15	$NaAlO_2$	2d hexagonal	HMI VPT	2d hexagonal	Amorphous	Sausage-like long chain

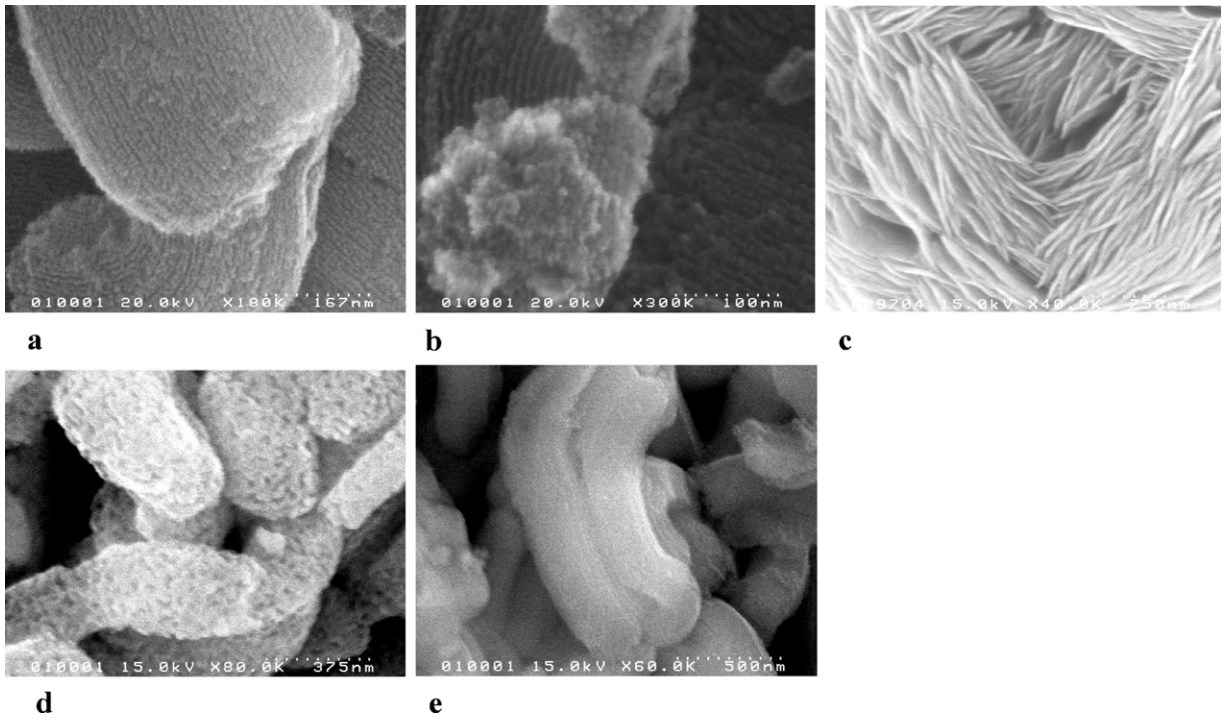

Fig. 2. SEM images of (a) parent SBA-15, (b) Al/SBA-15, (c) (b)+VPT7 days (MCM-22), (d) (b)+VPT5 days with less amount of H_2O, and (e) (b)+VPT7 days without H_2O (only HMI was supplied).

properties between MCM-22(P) crystallized by the hydrothermal method and by VPT with HMI and H_2O (Entries 1 and 2). As shown in Fig. 2, this assumption is supported by the morphology observed by SEM, where MCM-22 with a thin layered structure aggregates. Although Entry 3 suggests us that NaOH is not necessary to promote the nucleation of MCM-22, another experiment revealed that sodium aluminate was indispensable to form the phase. In any case, the morphology was drastically changed from the typical tube-like structure of SBA-15 into the typical one of MCM-22, and the formation of highly crystalline MCM-22 was confirmed. SBA-15 dehydrated at a higher temperature of 900 °C to lower the reactivity could also be utilized as the SiO_2 source for MCM-22 (Entry 4), and a dramatic change in the morphology of the product was still observed. In the case of the steam-assisted crystallization method (Entry 5), where only water vapor is supplied from the vapor phase to a solid including OSDA in a closed vessel, no crystalline phase was observed. Although the morphology resembled that of SBA-15, the mesostructure completely disappeared. Supplying only HMI from the vapor phase changed neither the ordered mesostructure nor the morphology of the parent SBA-15 (Entry 6), indicating that water vapor is critical in maintaining the mesostructure and crystallizing the zeolitic phase, i.e., in obtaining a composite material of MCM-22 with SBA-15-like mesostructure.

Fig. 3 illustrates the profiles for the temperature-programmed desorption (TPD) of toluene from sodium aluminate-containing SBA-15 (top) and from MCM-22 obtained through VPT of the sodium aluminate-containing SBA-15 (bottom). Only the peak assignable to the desorption of physisorbed toluene on/in the mesopores of SBA-15 was detected when Al/SBA-15 was applied. Another distinct peak, which appeared on the crystallized MCM-22 sample, can be assigned as a desorption peak of toluene trapped by the micropocket on the external surface of MCM-22. It is interesting to note that not only toluene but also benzene and cumene could be trapped by the same MCM-22, while 1,3,5-triisopropylbenzene and 2,2,4-trimethylpentane (isooctane) could not. These phenomena imply that the micropocket on the external surface of MCM-22 exhibits shape-selective adsorption of mono-alkylated aromatic compounds, which ultimately results in the unique shape-selective catalysis of MCM-22 for mono-alkylation of benzene into ethylbenzene or cumene.

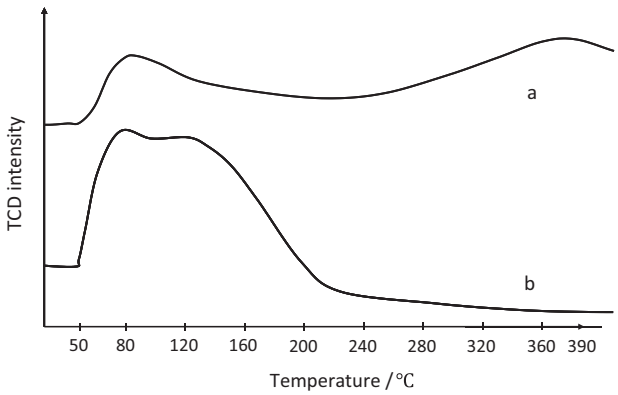

Fig. 3. Temperature-programmed desorption of toluene from (a) Al/SBA-15 and (b) (a)+VPT7 days (MCM-22).

What of the acidity of MCM-22 and its intermediate synthesized from SBA-15? Profiles of the TPD of ammonia from MCM-22, Al/SBA-15, and the products obtained under various conditions of VPT are demonstrated in Fig. 4. On MCM-22, a pair of distinct peaks was observed, in addition to a higher peak that could be recognized as desorbed ammonia from a zeolitic acid site. Aluminum-loaded SBA-15, which was ion-exchanged into the H form, had a broad peak that could not be separated from a low-temperature peak corresponding to physisorbed ammonia. Supplying a smaller amount of water vapor during VPT synthesis of MCM-22 from Al/SBA-15 led to a zeolitic desorption peak at a high temperature. Interestingly, only HMI without H_2O produced such a strong type of acid site on the sample, although it did not crystallize into a zeolitic phase. As seen in the XRD patterns of each sample, which are also displayed in the same figure, the ordered mesostructure of SBA-15 in the samples synthesized by VPT with less or without H_2O were retained and the diffraction could be observed. In contrast, samples obtained by normal VPT did not retain the ordered mesostructure. These results also indicate that water vapor supplied during synthesis by VPT plays a key role in the transformation of the amorphous mesoporous into the zeolitic phase.

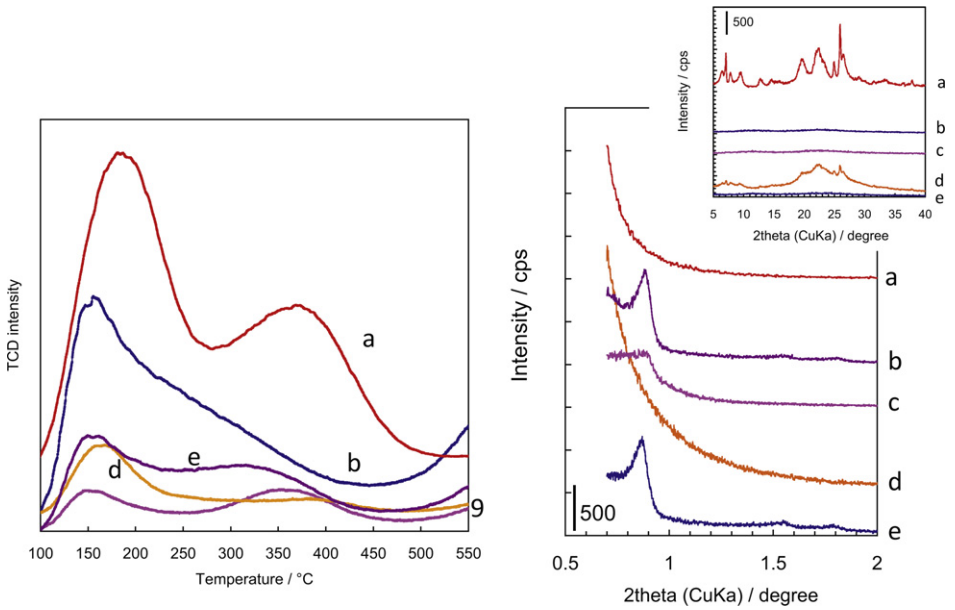

Fig. 4. Ammonia temperature-programmed desorption profiles and the XRD patterns of (a) Al/SBA-15+VPT7 days (MCM-22), (b) Al/SBA-15, (c) (b)+VPT7 days with less amount of H_2O, (d) (b)+VPT7 days with excess amount of H_2O, and (e) (b)+VPT7 days without H_2O (only HMI was supplied).

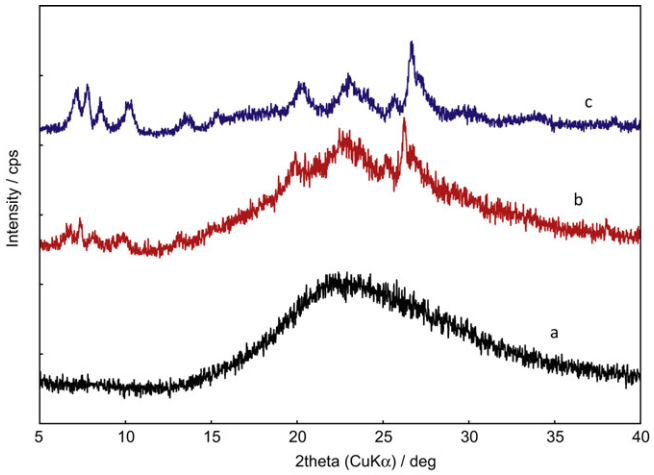

Fig. 5. XRD patterns of the sample after VPT synthesis for (a) 7 days, (b) 14 days, and (c) 21 days.

3.2. Phase transformation of amorphous mesoporous SBA-15 into zeolitic microporous MCM-22

In order to collect information on the phase transformation and to determine whether composites of MCM-22-type microporous and SBA-15-type mesoporous materials could be obtained, the intermediates at different stages of VPT were investigated in terms of long-range ordered structure (i.e., a building unit of MCM-22) and the location and environment of the acidic site on the sample. Fig. 5 shows the XRD patterns of the intermediates at 7, 14, and 21 days of VPT synthesis performed at a lower temperature to slow down crystallization. As can be observed, the long-range ordered structure began to form after at least 7 days of synthesis. Up to more than 20 days were required to crystallize the amorphous silicate into crystalline MCM-22. In contrast, the ordered mesostructure disappeared by 7 days of VPT crystallization.

The infrared spectra of these samples were collected to obtain information on when a building unit of zeolite is formed during synthesis, as shown in Fig. 6. The 21 day-VPT sample, which was fully crystallized into MCM-22(P), possessed unique doublet peaks at 560 and 610 cm^{-1}, which can be ascribed to the vibrations of a building unit of MCM-22. Another clear but broad absorption peak,

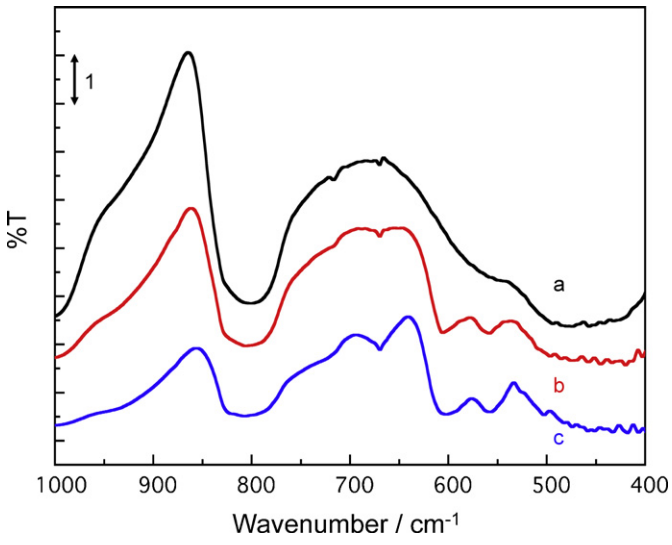

Fig. 6. Infrared spectra of the sample after VPT synthesis for (a) 7 days, (b) 14 days, and (c) 21 days.

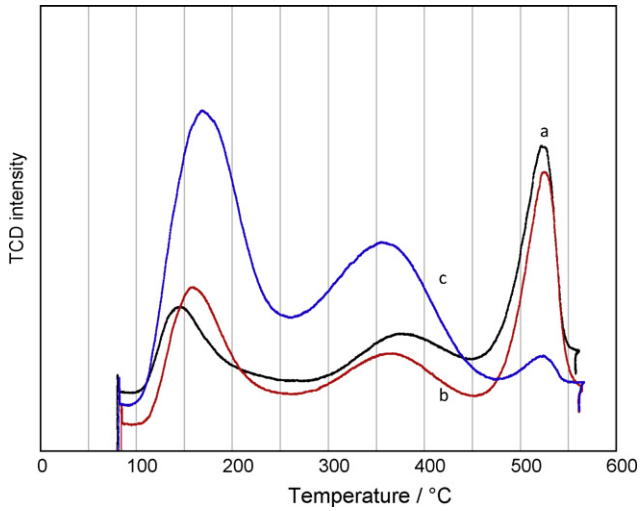

Fig. 7. Ammonia-TPD profiles of the sample after VPT synthesis for (a) 7 days, (b) 14 days, and (c) 21 days.

which is from amorphous silica, was detected at around 800 cm^{-1}. The intensity of the latter band decreased as the time of VPT synthesis increased, whereas the doublet peaks assignable to a building unit of MCM-22 began to increase in a similar way from the time when the diffraction could be detected. Therefore, it can be said that the building unit of the zeolite is already formed at a stage much earlier than that of full crystallization.

Changes around the acid site of the zeolite during the course of crystallization could be discussed by considering ammonia-TPD. Fig. 7 shows the profiles of ammonia desorbed from the samples. The peak at the highest temperature is due to water desorbed from the amorphous site of the sample, which decreased as the time of VPT increased. The peak corresponding to the desorption from the zeolitic acid site was changed quantitatively from 7 to 21 days of VPT. The peak point of the maximum rate of desorption was hardly changed, indicating that the acid site and its environment are already built up at an early stage of crystallization. The acidity of fully crystallized MCM-22 is almost comparable to that of the sample where the building unit of the zeolite is just formed.

As shown in Fig. 3, benzene and mono-alkylated benzenes such as toluene could be trapped in the micropocket on the external surface of MCM-22. The TPD of benzene was carried out to identify when the micropocket is generated during the course of crystallization. Fig. 8 summarizes the profiles of benzene-TPD from the samples with TG and *d*TG curves. As crystallization proceeded, the amount of benzene desorbed from the samples increased, mainly because a micropore developed. Zeolitic micropores are known to be effective for physically incorporating benzene. Judging from the *d*TG curve, the samples obtained after up to 14 days of VPT synthesis show one benzene desorption peak. After full crystallization of the sample into MCM-22, the profile of *d*TG involved a shoulder at a higher temperature, which was indicative of the benzene trapped in the micropocket of MCM-22 as in Fig. 3. These results also support the deduction that aromatic compounds are trapped, not chemically by the acidic character of zeolite, but rather physically by the zeolitic micropores.

As for the formation mechanism of the microstructure of MCM-22, we can say from the results obtained in this study that a zeolitic acid site similar to that of MCM-22 is generated at an early stage of crystallization, along with the formation of the building unit of the zeolite. Up to this stage, the mesostructure could be maintained; thus no dramatic changes in morphology of the parent SBA-15 took place. Therefore, a mesoporous silica with zeolitic acidity could be prepared by this method. Further crystallization

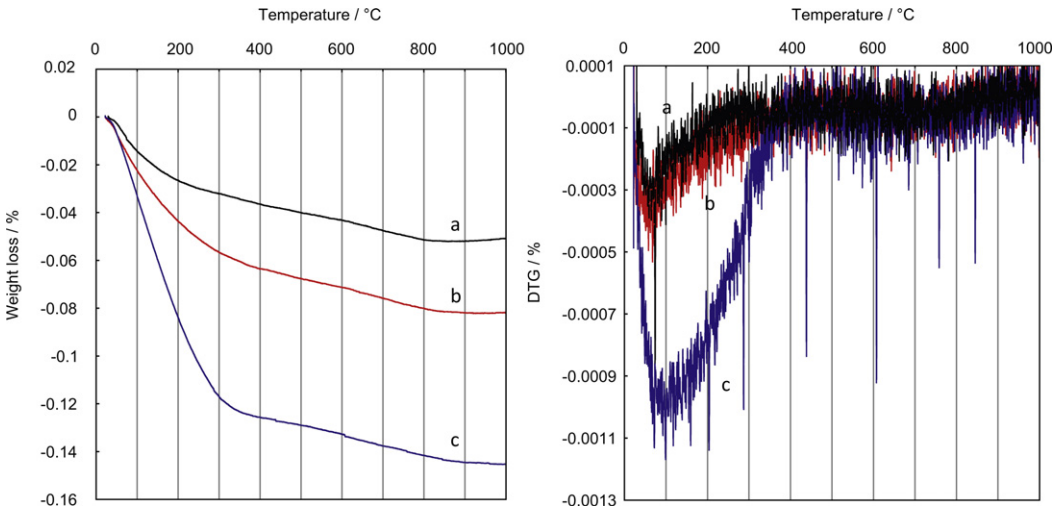

Fig. 8. Benzene-TPD profiles by thermogravimetry and its differential curve from the sample after VPT synthesis for (a) 7 days, (b) 14 days, and (c) 21 days.

at a later stage results in the formation of micropockets observed on the external surface of MCM-22, although the mesostructure and morphology of the original SBA-15 could not be sustained to this stage. The silica source might drastically reconstruct the surface from an amorphous to a crystalline structure—a process which can be accelerated with the help of water vapor. In conclusion, a composite of micro- and mesoporous structures derived from MCM-22 and SBA-15, respectively, is difficult to obtain through this method, especially without mesostructural supports such as carbon inside the mesopores.

4. Conclusions

In order to obtain a micro- and mesoporous composite material in its true sense, a partial transformation of the mesoporous amorphous silica wall of SBA-15 into microporous MCM-22 was carried out by a dry gel conversion technique known as vapor-phase transport. Although the direct preparation of a micro- and mesoporous composite was unsuccessful, it was found that slow conversion into zeolitic crystalline aluminosilicate, as well as mesostructural supports such as carbon inside the mesopores of SBA-15, are quite important for the successful preparation.

As aspects of the formation mechanism of MCM-22, it was found that micropockets on the external surface of MCM-22 require a long period of crystallization, and that a building unit of MCM-22 and the environment of a zeolitic strong acid site are generated at an early stage of crystallization. Therefore, by consideration of the formation mechanism, a composite material with a mesostructure and a zeolitic strong acid site is expected to be readily formed through the VPT method.

References

[1] M. Ogura, Catal. Surv. Asia 12 (2008) 16.
[2] K.R. Kloetstra, H. van Bekkum, J.C. Jansen, Chem. Commun. (1997) 2281.
[3] A. Karlsson, M. Stocker, R. Schmidt, Micropor. Mesopor. Mater. 27 (1999) 181.
[4] L. Huang, W. Guo, P. Deng, Z. Xue, Q. Li, J. Phys. Chem. B 104 (2000) 2817.
[5] Y. Liu, W. Zhang, T.J. Pinnavaia, J. Am. Chem. Soc. 122 (2000) 8791.
[6] Z. Zhang, Y. Han, L. Zhu, R. Wang, Y. Yu, S. Qiu, D. Zhao, F.-S. Xiao, Angew. Chem. Int. Ed. 40 (2001) 1258.
[7] D.T. On, S. Kaliaguine, Angew. Chem. Int. Ed. 40 (2001) 3248.
[8] C.S. Carr, S. Kaskel, D.F. Shantz, Chem. Mater. 16 (2004) 3139.
[9] S.I. Cho, S.D. Choi, J.-H. Kim, G.-J. Kim, Adv. Funct. Mater. 14 (2004) 49.
[10] Y. Zhang, T. Okubo, M. Ogura, Chem. Commun. (2005) 2719.
[11] M. Choi, H.S. Cho, R. Srivastava, C. Venkatesan, D.-H. Choi, R. Ryoo, Nat. Mater. 5 (2006) 718.
[12] Y. Fang, H. Hu, J. Am. Chem. Soc. 128 (2006) 10636.
[13] M. Choi, K. Na, J. Kim, Y. Sakamoto, O. Terasaki, R. Ryoo, Nature 461 (2009) 246.
[14] M. Matsukata, M. Ogura, T. Osaki, P.R.H.P. Rao, M. Nomura, E. Kikuchi, Top. Catal. 9 (1999) 77.
[15] M.E. Leonowicz, J.A. Lawton, S.L. Lawton, M.K. Rubin, Science 264 (1994) 1910.
[16] A. Corma, V. Martinez-Soria, E. Schnoeveld, J. Catal. 192 (2000) 163.
[17] S. Inagaki, K. Kamino, M. Hoshino, E. Kikuchi, M. Matsukata, Bull. Chem. Soc. Jpn. 77 (2004) 1249.